Available online at www.sciencedirect.com
SCIENCE DIRECT®

Journal of Catalysis 228 (2004) 397–404

JOURNAL OF CATALYSIS

www.elsevier.com/locate/jcat

Oxidation catalysis of unsaturated hydrocarbons with molecular oxygen via single-electron transfer in thermally treated H zeolites

Thomas M. Leu, Emil Roduner *

Institut für Physikalische Chemie der Universität Stuttgart, Pfaffenwaldring 55, D-70569 Stuttgart, Germany

Received 19 May 2004; revised 2 September 2004; accepted 6 September 2004

Available online 28 October 2004

Abstract

An electron spin resonance investigation demonstrates that radical cations in dehydroxylated zeolites are intermediates of a catalytic oxidation reaction that consumes molecular oxygen and involves radical cation transients of unsaturated hydrocarbons. Radical cation generation has often been attributed to the action of Lewis acid sites, generated by a thermal treatment of a proton-exchanged zeolite. The present study of the conditions for radical cation generation and stabilization shows that the active centers are nonacidic, which means that separate special single-electron redox-active catalytic sites are present in the zeolite. Simultaneous monitoring by ESR of the organic radical cation, the superoxide radical anion, and molecular oxygen in the reaction of 2,5-dimethylhexa-2,4-diene with O_2 in dehydroxylated H-MOR revealed in one case more than 4000 cycles per active center, demonstrating their catalytic activity.

© 2004 Published by Elsevier Inc.

Keywords: Acidic zeolite; Dehydroxylation; Lewis acid site; Radical cation; Single-electron transfer; Hydrocarbon oxidation

1. Introduction

Brønsted acid sites (BAS) in the H form of zeolites have been well characterized and are generally thought to involve bridging hydroxyl groups, Si–O(H)–Al [1–3]. Depending on the postsynthesis treatment the H form of zeolites also contains Lewis acid sites (LAS). They develop from BAS by elimination of water at temperatures above approximately 623 K. This dehydroxylation leads to a threefold coordinated silicon atom with a positive charge and a threefold coordinated aluminum atom which is called Lewis acid site because it is coordinatively unsaturated and interacts strongly with bases [4,5]. Others suggested that there are no unsaturated aluminum atoms in the lattice and proposed the existence of ions like AlO^+, located at cation positions, as the real sites created by the dehydroxylation process [6–8]. These species were called “True Lewis Sites.” There is general agreement that in the presence of traces of water thermally treated H zeolites develop some kind of aluminum oxide ions or clusters outside of regular lattice positions or even amorphous aluminum oxide phases, but the exact nature of LAS is still a matter of debate since they are elusive to direct spectroscopic observation. A comprehensive review has been given by Kühl [9].

One of the most intriguing properties of acid zeolites is their ability to generate spontaneously ESR-active radical cations from unsaturated hydrocarbons, in particular condensed aromatic hydrocarbons but also aliphatic and cyclic olefins (see, e.g., [10]). There is limited experimental information on the nature of the active sites of single electron oxidation since the transferred electron is ESR silent in zeolites. The common opinion is that LAS are responsible [11]. A hydrothermal treatment of the H form seems to be a necessary condition. Radical cations are not formed in the Na form except from hydrocarbons with very low ionization potentials [12]; they are also not observed with aluminum-free materials like Silicalite-I. Furthermore, molecular oxygen seems to play an active role [10], but radical cations have also been obtained under argon [10] so that the exact role of

---

* Corresponding author. Fax: +49 711 685 4495.
E-mail address: e.roduner@ipc.uni-stuttgart.de (E. Roduner).

0021-9517/$ – see front matter © 2004 Published by Elsevier Inc.
doi:10.1016/j.jcat.2004.09.008

oxygen is not clear. Most authors assume that chemisorbed oxygen enhances the activity of the Lewis acid sites, others postulate the generation of positively charged oxygen species like $O^{+\bullet}$ [13] or $O_2^{+\bullet}$ [14] in a high-temperature reaction.

Molecular oxygen also acts as a single-electron acceptor and leads to the formation of the superoxide radical anion ($O_2^{-\bullet}$) when the gas is added to a zeolite which already contains radical cations [15,16]. This secondary-electron transfer also takes place with other substrates with a high electron affinity, such as tetracyanoethene [16]. It has been suggested that O_2 may serve as the final electron sink which renders the overall process catalytic [10]. Free radicals play a role in coke deposition which represents a severe problem in many acid-catalyzed processes [17,18]. Radical cations are possibly involved in catalytic cracking reactions [19] but we are not aware of any catalytic process in acidic zeolites with neutral free radical intermediates in the conversion of hydrocarbons.

The present investigation into single-electron transfer and the active sites involved is a continuation and full account of a preliminary communication [20]. It first focuses on the optimum conditions for the generation of radical cations in the zeolites H-mordenite (H-MOR) and H-ZSM-5 (Section 3.1). Then the nature of the active sites and the role of molecular oxygen in single-electron transfer processes is studied (Section 3.2). Finally, the backtransfer of single electrons to gaseous oxygen was investigated. We conclude that single-electron oxidation is initiated by catalytically active sites (Section 3.3), and we demonstrate that both single-electron transfers are included in a catalytic cycle. In the future this might lead to a novel and environmentally benign approach for the catalytic oxidation of unsaturated hydrocarbons.

2. Experimental

The Na form of the zeolites (with a molar ratio of $(SiO_2/Al_2O_3) = 12$ and a crystal size of about 1–2 µm in the case of Na-mordenite, or with a molar ratio of $(SiO_2/Al_2O_3) = 40$ and a crystal size of about 0.2–1 µm in the case of Na-ZSM-5, respectively) was supplied by CU Chemie Uetikon AG, Uetikon, Switzerland. The raw materials were proton-exchanged three times with a 10-fold excess of NH_4NO_3 ($1\ \mathrm{mol\,L^{-1}}$) at 353 K in the case of Na-MOR, or with HCl ($0.1\ \mathrm{mol\,L^{-1}}$) at room temperature in the case of Na-ZSM-5, respectively, and predried at 363 K after washing. Calcination was carried out at 973 K (using a heating rate of $100\ \mathrm{K\,h^{-1}}$), either in air or in vacuum for 15 h, unless otherwise stated. The subsequent preparation steps were performed using an all-steel adsorption system capable of reaching a vacuum of 10^{-7} hPa. The calcined zeolites were degassed in ESR tubes at temperatures up to 573 K in a dynamic vacuum of at least 10^{-6} hPa, measured near the vacuum pump, which corresponds to less than 10^{-4} hPa measured directly on top of the ESR tube. Liquid hydrocarbons, previously degassed by freeze-pump-thaw cycles, were vacuum-distilled onto the zeolite at room temperature; O_2 was used directly. The adsorption process was monitored using pressure sensors (Kobold Messring GmbH, Hofheim/Ts., Germany, and STS AG, Sirnach, Switzerland). The loading of 2,5-dimethylhexa-2,4-diene (DMHD) was usually adjusted to a range of 0.5 to 2.5% (w/w) which corresponds to 0.15 to 0.7 molecules per unit cell.

The emerging radical cations were observed using an ESR spectrometer (Bruker EMX series) operating at X-band frequency. Quantitative measurements of ESR signals were related to a weak pitch standard.

The decay products of the DMHD radical cation were determined by a GC/MS system (Agilent Technologies GC Model 6850 Plus coupled with a Model 5973 mass-selective detector). Mass spectra were interpreted with the help of the mass spectral library NIST ’98. The exact mass of relevant parent ions was determined using a high-resolution mass spectrometer (Finnigan MAT 95) to confirm the assignment of some peaks in the total ion chromatograms.

3. Results and discussion

3.1. Generation of the DMHD radical cation

2,5-Dimethylhexa-2,4-diene offers several advantages for probing the electron, accepting capabilities of zeolites:

(i) The radical cation of DMHD is relatively long lived.
(ii) The gas-phase ionization potential of DMHD amounts to only 7.9 eV [21]. In the polarizing environment of a zeolite pore it is further reduced [10]. Radical cations with high ionization potentials tend to transform quickly into more stable ones, which complicates spectroscopic analysis. Due to the high stability of $DMHD^{+\bullet}$ we never observed its transformation into other ESR visible species.
(iii) $DMHD^{+\bullet}$ shows a well-resolved ESR spectrum with narrow lines in H-MOR (Fig. 1a). It is therefore easily distinguished from superimposed spectra of other radicals which are usually much broader. The exceptionally narrow lines are due to a high mobility of the radical cations in the mordenite channels, which results in a relatively small anisotropy of the hyperfine coupling tensors. The spectrum was analyzed in depth previously [22].

The diffusivity of the diene is high in mordenite, and the distillation of a small amount of it into an ESR tube containing the zeolite powder leads to the evolution of the ESR signal of $DMHD^{+\bullet}$ in all regions of the powder within about 15 min, even if the zeolite bed measures more than 10 cm in height. We therefore assume that DMHD can access any active electron-accepting site within the mordenite channels.

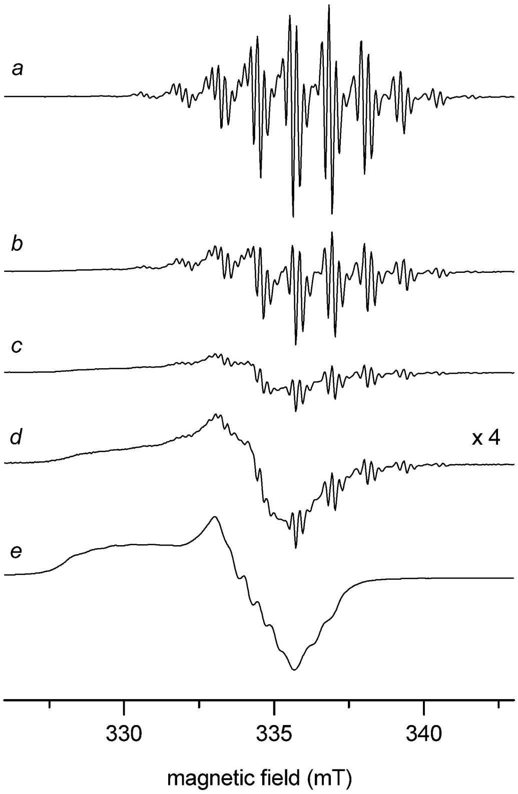

Fig. 1. ESR spectra of air calcined H-MOR with adsorbed DMHD, immediately before the addition of oxygen (a), and subsequently exposed to oxygen with a partial pressure of 52 hPa, recorded 2 min (b), 36 min (c), and 100 min (d) after addition of the oxygen. ESR spectrum of the superoxide radical anion, formed upon addition of 250 hPa of oxygen to a different DMHD-loaded samples of H-MOR, measured some days after oxygen addition (e).

Counterdiffusion is possible in mordenite for benzene and ethylbenzene [23]. Their cross section is comparable or even greater than that estimated for DMHD molecules, one may therefore assume that DMHD molecules can pass each other in mordenite pores.

ESR spectra obtained with DMHD in H-ZSM-5 were not as well resolved as in H-MOR. This is ascribed to a considerably restricted motion in the medium-pore zeolite. It makes it much more difficult to quantify radical cation generation: We will therefore concentrate here on the results obtained with H-MOR, but all the main features were observed with H-ZSM-5 as well.

HCl leads to extensive dealumination of H-MOR [24, 25], causing partial pore blockage by extraframework aluminum oxide. Better yields of DMHD$^{+\bullet}$ are obtained with NH_4NO_3 which does not cause measurable dealumination [26]. This indicates that an extractive dealumination is apparently not needed to generate radical cations. Provided that the migration of aluminum atoms is necessary for the creation of single-electron-accepting centers, it is sufficient to perform calcination under self-steaming conditions in a shallow bed (see Section 3.2).

The maximum concentration of DMHD$^{+\bullet}$ is mostly reached within 10 to 15 min after the adsorption of the hydrocarbon. This time depends mainly on the residual humidity in the zeolite channels; it is higher for less thoroughly dried samples. The half-life usually amounts to slightly less than an hour at room temperature. Since CW ESR is a rather slow method a lifetime of this order is impractical. The lifetime raises when the zeolite is loaded with greater amounts of the hydrocarbon, but this is at cost of spectral resolution due to a reduction of the dynamics of the guest species in the crowded channels. We take this finding as a hint that diffusion processes control the fading of the radical cation signal.

3.2. Active sites for single-electron transfer

3.2.1. The role of oxygen for the generation and activation of oxidative sites

Calcination was performed under shallow bed (2 mm) conditions in flowing air in a horizontal quartz tube. After transfer into an ESR tube and subsequent evacuation and loading with the hydrocarbon, a radical cation concentration of $6 \times 10^{-8}\ \mathrm{mol\,g^{-1}}$ (±25%) was obtained.

Alternatively, to evaluate the role of the oxygen, samples were carefully dried in an ESR tube under deep-bed conditions (80 mm) by evacuation at room temperature for 24 h and then heating at a rate of $3\ \mathrm{K\,min^{-1}}$ up to 773 K, keeping this temperature for 2 h, and evacuating for another 12 h at room temperature to reach a pressure of 3×10^{-7} hPa. After this initial drying calcination was conducted as usual, except that the sample was kept under vacuum. This resulted in a radical cation concentration of $2.4 \times 10^{-8}\ \mathrm{mol\,g^{-1}}$ in the middle of the zeolite bed (about 40% of what was observed in air calcined samples). However, the top and bottom layers were nearly inactive. Presumably, the top layer resembles a fully dehydroxylated zeolite. In the deeper parts of the powder the effective vacuum is much poorer. A certain extent of “steaming” with low water vapor pressures arising from dehydroxylation is necessary for the evolution of electron-accepting centers, but in this lower part the water content may be too high and cause more significant dealumination and possibly also pore blockage.

In the intermediate zone of the vacuum-calcined zeolite it is possible to enhance the radical cation signal by a supplementary addition of oxygen to a concentration which is comparable to the value observed after calcination in air. This clearly demonstrates that oxygen plays an important role in electron transfer.

ESR spectroscopy has the advantage that gaseous triplet oxygen is detectable within a certain pressure range. The interaction of the rotational and the orbital angular moments with the magnetic spin moment leads to a multitude of individual lines. The single scan detection limit in an empty ESR tube is around 10^{-3} hPa. Oxygen rotates freely in mordenite above 200 K [27], but the lifetime of a molecular rotational state in the pore is too short for the molecule to be detectable by ESR. Nevertheless, the presence of intergranular oxygen

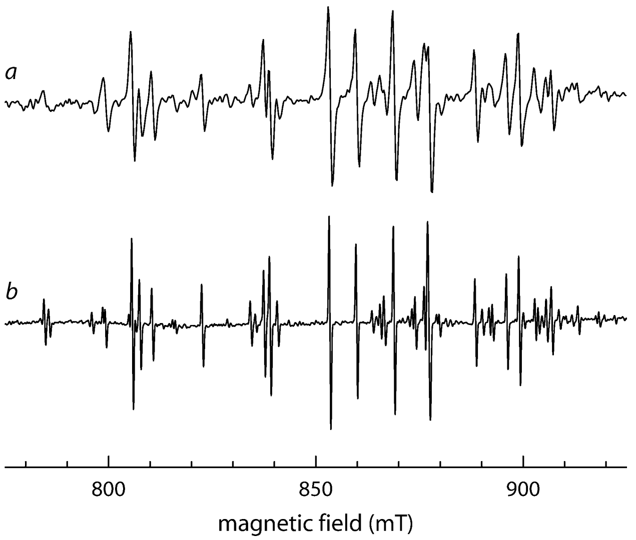

Fig. 2. ESR spectrum of the lower part of a layer of H-MOR after a usual drying and evacuating procedure (a), obtained with five CW scans and resolution enhanced by multiplying the inverse Fourier-transformed spectrum with a sinebell function. For comparison, spectrum (b) shows the resonance lines of gaseous oxygen with a pressure of 5×10^{-2} hPa, scaled down to the same height.

in equilibrium with the adsorbed state permits its observation at room temperature with only slightly broadened lines, as shown in Fig. 2. By comparing the ESR intensities of a calibration series with our samples we established that a pressure of the intergranular oxygen in a range of 10^{-3} to 10^{-2} hPa is best for generating a large quantity of DMHD radical cations. Higher pressures lead to the additional evolution of superoxide ions (see Section 3.3).

3.2.2. *ESR investigations with and without probe molecules*

The concentration of active sites for $\mathrm{DMHD}^{+\bullet}$ generation is much too low to be detectable by NMR. Basically, ESR spectroscopy should be sufficiently sensitive, but in fact only the radical cations were observed. Nobody has been able to detect directly the active centers.

Ammonia interacts with all kinds of acid sites including the weak ones which are not catalytically active. Ammonia adsorption therefore provides an upper threshold for acidic centers in zeolites [28,29]. Its adsorption enthalpies amount to more than 120 $\mathrm{kJ\,mol^{-1}}$ for strong acid centers and between 100 and 120 $\mathrm{kJ\,mol^{-1}}$ for weak ones. Strong centers with adsorption enthalpies of more than 120 $\mathrm{kJ\,mol^{-1}}$ are ascribed to LAS arising from dehydroxylation and dealumination [30–32]; cationic LAS such as $\mathrm{Na^+}$ do not significantly interact with ammonia [33,34].

From ammonia adsorption a total of approximately 0.8 acidic centers per unit cell was determined for our calcined H-MOR samples, compared to nominally 7 per unit cell in the original H form. The reduced concentration is due to partial transformation of BAS into LAS and corresponds well with related literature data [35].

Complexation of the acid sites before or after admission of DMHD revealed no influence of ammonia for the development of $\mathrm{DMHD}^{+\bullet}$. While it was found previously that radical cations are also formed on zeolites in their $\mathrm{NH_4}^+$ form [36], ammonia was not present in excess in that experiment so that there was no possibility of blocking the LAS. From the present results we conclude that single-electron transfer and acid–base interaction take place at different adsorption sites, and neither LAS nor BAS are directly involved in the single-electron transfer process. It also suggests that it is essential to distinguish between the acidic and the redox active properties. This is consistent with the conventional definition that Lewis acid sites are electron pair acceptors whereas the formation of radical cations represents the transfer of single electrons. We therefore call these separate sites which are responsible for radical cation generation single-electron transfer sites (SETS).

The presence of SETS is obviously linked to moderate steaming during calcination and thus to the formation of defect sites. The formation of oxygen vacancies at temperatures above 643 K in H-ZSM-5 was demonstrated recently by Balint et al. [37] based on AC conductivity that scaled as $p_{\mathrm{O_2}}^{1/4}$. While this is typical for many ionic solid oxides [38], it has not frequently been proposed to occur in zeolites. However, as the activity of the SETS in the present work on H-MOR obviously depends on the partial pressure of oxygen we believe that the SETS are indeed related to oxygen vacancies. In the absence of direct spectroscopic evidence it remains somewhat speculative but is nevertheless an attractive approach for understanding the nature of these centers.

In a detailed investigation of the oxidation of benzene to phenol with $\mathrm{N_2O}$ over steamed H-ZSM-5 Kubánek et al. [39] demonstrated that the catalytic activity was uncorrelated with the number of BAS or LAS but clearly correlated with relatively low concentrations of Fe in the zeolite, and they implied that the ESR signals near $g = 6.0$ and 5.6 arising from extra-framework Fe(III)-oxo cations in highly distorted coordination were particularly important for the hydroxylation activity. There was no evidence of radical cation formation. In the present work, while the ESR signal at $g = 4.3$ which is typical for Fe in near-tetrahedral coordination was always present we did not observe any signals at higher g values; instead, there was a prominent signal of radical cation intermediates. These clear differences seem to indicate that the Fe-oxo species in Kubánek's work may not be the same as the SETS sites needed for the present study.

3.3. *The catalytic action of SETS in the oxidation of unsaturated hydrocarbons*

3.3.1. *In situ ESR spectroscopic observation of the reaction of the DMHD radical cation with oxygen*

Oxidation activity of zeolites has been described for a number of reactions involving oxygen or nitroxides as oxidizing agents [10,39]. It is also not new that superoxide radical anions are formed [16]. A photocatalytic oxidation process developed by Blatter, Frei and co-workers [40–42] using hydrocarbons (HC) and molecular oxygen on cation-exchanged zeolites was postulated to lead to radical cations and superoxide radical anions as reaction intermediates:

$$[\mathrm{HC}\cdot\mathrm{O_2}] \overset{(h\nu)}{\rightleftharpoons} [\mathrm{HC}^{+\bullet}\cdots\mathrm{O_2^{-\bullet}}]^* \rightarrow \mathrm{HC}^{+\bullet} + \mathrm{O_2^{-\bullet}} \rightarrow \text{products.}$$

As products, these authors detected hydroperoxides in high selectivities by IR spectroscopy. Here we focus on a very similar reaction in the absence of UV activation, and we demonstrate that it is catalytic and can have a high turnover number.

Addition of molecular oxygen to a calcined zeolite containing radical cations of unsaturated hydrocarbons leads to a reaction of the guest species, provided the oxygen pressure exceeds a certain limit. This limit was not determined exactly, but it was established that a partial pressure of 0.5 hPa is sufficient but 10^{-2} hPa does not lead to a transformation of the DMHD radical cations. The reaction can be monitored by ESR spectroscopy because it results in the formation of superoxide radical anions due to a backtransfer of the unpaired electrons from the SETS to oxygen molecules.

Superoxide ions adsorbed on the surfaces of solid oxides have been characterized in depth by ESR [43]. Their signal is quite broad and shows a low resolution in most environments. Because of the far higher resolution the $\mathrm{DMHD}^{+\bullet}$ signal is well distinguishable from the broad features of $\mathrm{O_2^{-\bullet}}$. The g and hyperfine tensors of $\mathrm{O_2^{-\bullet}}$ are resolved (see Fig. 1e) and were analyzed previously [20]. The splitting of each component into six lines shows that the superoxide ions are adsorbed in the neighborhood of aluminum atoms which posses a nuclear spin of $I = 5/2$. The coupling constants agree well with literature data [44]. These aluminum atoms have to exist in a coordinatively unsaturated form in the lattice or in amorphous $\mathrm{Al}_x\mathrm{O}_y$ phases which have been postulated to be formed in calcined as well as in hydrothermally treated zeolites. Presumably, these aluminum sites are responsible for the back transfer of the single electrons.

In the following we report three experiments with well-defined amounts of zeolite, DMHD, and $\mathrm{O_2}$ in sealed quartz tubes which permit a simultaneous monitoring of $\mathrm{DMHD}^{+\bullet}$, $\mathrm{O_2^{-\bullet}}$, and $\mathrm{O_2}$ and give insight into the reaction of the system H-MOR/$\mathrm{DMHD}^{+\bullet}$ with oxygen. In the first experiment a sample of H-MOR was calcined in air and afterward loaded with DMHD. The ESR signal of the corresponding radical cation is shown in Fig. 1a. After recording this spectrum, oxygen was added with a partial pressure of 52 hPa. Immediately thereafter, a second spectrum (b) was taken which shows that the number of radical cations has diminished. At the same time, the broad superimposed superoxide anion signal evolved. With time, the signal of the anion clearly dominates the spectrum whereas the signal of the cation fades away (spectra (c) and (d)). The cation signal never vanishes entirely, even after weeks, although it adopts a very small amplitude.

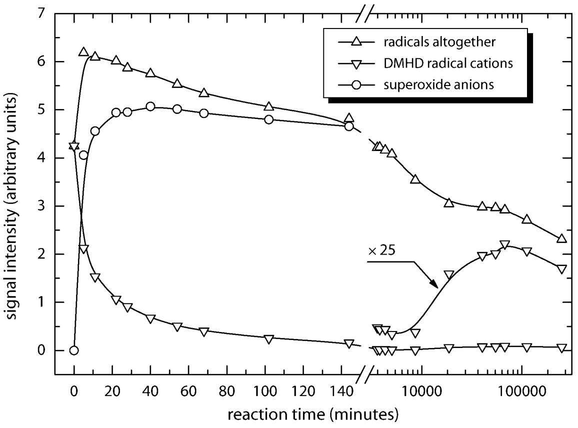

Fig. 3. Quantitative analysis of the relative concentrations of all radical species in the system H-MOR/$\mathrm{DMHD}^{+\bullet}/\mathrm{O_2}$ (first described experiment; some spectra of this set are shown in Fig. 2).

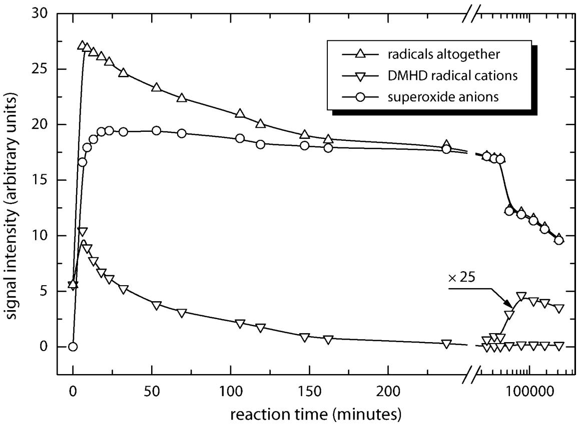

Fig. 4. Quantitative analysis of the relative concentrations of all radical species in the system H-MOR/$\mathrm{DMHD}^{+\bullet}/\mathrm{O_2}$ (vacuum-calcined zeolite) in the second experiment described in the text with 68 hPa of added oxygen.

A quantitative analysis of the ESR signal intensity of both radical species is shown in a diagram monitoring intensity over time in Fig. 3. The left side of this diagram (up to a reaction time of 2.5 h) shows the decrease of $\mathrm{DMHD}^{+\bullet}$ after adding the oxygen as well as the evolution of $\mathrm{O_2^{-\bullet}}$. The concentration of the latter species is about constant in the further course of the reaction. A short time after adding the oxygen the total concentration of radicals reaches a maximum which roughly corresponds to the maximum concentration of $\mathrm{DMHD}^{+\bullet}$ before its reaction with oxygen. The right-hand side of the diagram will be discussed later.

A second experiment differed from the first in that calcination was performed in vacuo at 973 K for 15 h under deep-bed conditions in the ESR tube. Exposure to an oxygen pressure of 68 hPa after addition of DMHD leads to a significant increase of the initial radical cation concentration (Fig. 4). Simultaneously the superoxide anion develops, and again a few minutes later a nearly constant concentration of

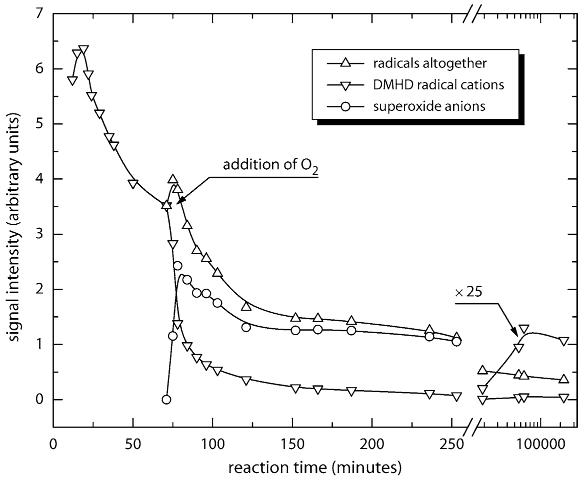

Fig. 5. Quantitative analysis of the relative concentrations of all radical species in the system H-MOR/DMHD$^{+\bullet}$/O$_2$ (air-calcined zeolite) in the third experiment described in the text with 24 hPa of added oxygen.

this species is observed. The initial increase in DMHD$^{+\bullet}$ concentration turns into a decease after about 10 min.

In a third experiment we used again an air-calcined sample of H-MOR. After the DMHD$^{+\bullet}$ signal had fully developed oxygen was added with a partial pressure of 24 hPa. In this case one finds a very strong decrease in DMHD$^{+\bullet}$ concentration after a short reaction time, as shown in Fig. 5. Besides this, the concentration of the superoxide ions is quite low and does not anymore reach the initial DMHD$^{+\bullet}$ concentration. This experiment shows that the extent of electron backtransfer from the zeolite lattice depends on the oxygen pressure. In contrast, the rate of decrease of DMHD$^{+\bullet}$ is not affected by the oxygen pressure.

After some hours of reaction time the concentrations of the radical species in all experiments hardly changed anymore. The amount of DMHD$^{+\bullet}$ stabilizes at a very low level. However, after some days or weeks, depending on the amount of added oxygen, a noticeable increase was detected, accompanied by a simultaneous decrease in superoxide anion concentration. The increase in DMHD$^{+\bullet}$ concentration was significant, although the initial values were not reached by far. The effect is seen in all of the intensity diagrams (Figs. 3, 4, and 5) on the right-hand side. It reflects quite a steep ascent followed by a slow and final decrease (note the logarithmic time scale).

The decline of the radical cation concentration after addition of oxygen is clearly the result of a chemical reaction into ESR-invisible reaction products. Furthermore we established that the DMHD$^{+\bullet}$ increase after long times always took place exactly when all of the added oxygen was used up. (It is possible to monitor the consumption of molecular oxygen in a range from 1 to 100 hPa concurrently with the radical species by means of ESR in X-band by analyzing the width of individual lines. The simplest way to do this is to compare the spectra of interest with a series of reference spectra, as reported previously [20].)

It is important to point out that in all experiments the molar amount of oxygen was many times the initial amount of the radical cation, but only a fraction of the amount of the parent hydrocarbon. The evolution of the concentrations of all three radical species is explained on the following basis:

(i) The reaction between the two radical ions leads to a closed-shell reaction product.
(ii) The electron transfer at the active sites of the zeolite is reversible and takes place repeatedly.

In other words, the SETS are catalytically active with respect to single-electron transfer. This explains not only the increase of radical cation concentration simultaneously with the decrease of radical anion concentration but also that a small quantity of DMHD radical cations is always present during the reaction with oxygen. It is obvious that such a catalytic process enables the reaction of the hydrocarbon with oxygen at room temperature, a reaction that is not possible under these gentle conditions in the absence of a catalyst. The catalytic cycle is illustrated in the reaction scheme [20]:

$$\mathrm{DMHD} + \mathrm{SETS} \rightarrow \mathrm{DMHD}^{+\bullet} + \mathrm{SETS}^{-\bullet} \tag{1}$$

$$\mathrm{SETS}^{-\bullet} + \mathrm{O_2} \rightarrow \mathrm{SETS} + \mathrm{O_2^{-\bullet}} \tag{2}$$

$$\mathrm{DMHD}^{+\bullet} + \mathrm{O_2^{-\bullet}} \rightarrow \text{products} \tag{3}$$

$$\mathrm{DMHD} + \mathrm{O_2} \rightarrow \text{products} \tag{1–3}$$

After complete oxygen consumption, SETS which are still accessible to DMHD molecules continue to form radical cations, but they do no longer find superoxide anions to react with, which leads to the described increase of their concentration.

The same effect is observed when the catalytic reaction is stopped at an early stage by removing the oxygen through application of vacuum. Within a few minutes the radical cation concentration raises and the magnitude of this immediate increase depends on how thoroughly the oxygen is removed.

It is obvious from the diagrams in Figs. 3, 4, and 5 that except during the induction period the concentration of superoxide anions clearly exceeds that of radical cations so that a simple charge balance in the form

$$c_{\mathrm{DMHD}^{+\bullet}} = c_{\mathrm{SETS}^{-\bullet}} + c_{\mathrm{O_2^{-\bullet}}}$$

is not valid, not even in case of a negligible concentration of the invisible SETS$^{-\bullet}$. This is possible when the above reaction scheme is extended by a bimolecular termination of DMHD$^{+\bullet}$ which transforms the radical cations to diamagnetic products and protons. The disappearance of DMHD$^{+\bullet}$ in the absence of oxygen indeed appears to follow second order kinetics (not shown).

Table 1
Molar amounts and concentrations of all observed species in the reaction of the system H-MOR/DMHD$^{+\bullet}$ with oxygen, together with relevant figures describing the catalytic activity of the SETS

Experiment[a]	Unit	A	B	C	D	E
Preparation method[b]		A	A	V	V	A
Weight of zeolite sample	mg	189	166	165	130	165
Concentration of DMHD$^{+\bullet}$ [c]	10^{16} g^{-1}	2.96	3.07	2.94	1.11	1.90
	10^{-8} mol g^{-1}	4.92	5.09	4.88	1.85	3.16
	10^{-4} (u.c.)$^{-1}$	1.42	1.47	1.41	0.53	0.91
Adsorbed amount of DMHD	µmol	34.3	25.1	29.9	58.5	45.0
	(u.c.)$^{-1}$	0.52	0.43	0.52	1.31	0.79
Converted amount of O_2	µmol	5.22	1.92	3.37	9.95	1.11
Starting pressure of O_2	hPa	260	52	68	337	24
Reaction time[d]	days	218	6.5	20	172	12
Number of cycles	–	562	226	419	4173	213
TON (turnover number)	h^{-1}	0.11	1.45	0.87	1.01	0.74
TOT (turnover time)	h	9.31	0.69	1.15	0.99	1.35
	min	559	41	69	59	81

[a] The time-dependent quantitative evaluation of the radical species is given in Fig. 3 for experiment B, in Fig. 4 for experiment C, and in Fig. 5 for experiment E.

[b] "A" designates shallow bed calcination in air, "V" stands for a vacuum calcination in the ESR tube under deep-bed conditions.

[c] Maximum number of radical cations, determined during the initialization period of the system H-MOR/DMHD$^{+\bullet}$ before addition of oxygen, related to the dehydrated form of H-MOR, "u.c." designates a unit cell of the zeolite.

[d] Time measured up to the entire consumption of the intergranular oxygen gas.

3.3.2. Quantitative evaluation of the SETS activity

For the purpose of quantitative evaluation of the above catalytic system we carried out five experiments in which we added defined amounts of oxygen and established the necessary time to completely turn over the oxidant. The samples were kept in the dark at room temperature. The number of consumed oxygen molecules per unit time divided by the number of available active sites (approximated by the maximum number of DMHD$^{+\bullet}$ after adsorption of the olefin) is the turnover number (TON). The results are given in Table 1, along with the preparation method of the sample, the molar amounts of the reactants, and the total turnover.

The TON amounts to approximately 1.1 h^{-1} on average in experiments B to E. Obviously it makes no difference whether the zeolite was calcined in air or in vacuo. Only in experiment A we established a much lower turnover per time. In contrast to the other experiments, sample A was prepared in an ESR tube with a smaller diameter (2 mm instead of 2.75 mm) resulting in a higher layer of the zeolite powder in this tube (80 mm instead of 40 mm in samples B to E). This may have lead to a less effective drying and therefore to a greater remaining humidity in the sample.

Considering the early state of our experiments the observed number of reaction cycles is remarkable. It is especially noteworthy that even more than 4000 turnovers do not lead to a deterioration in catalyst activity. It is therefore at this point not necessary to worry about coke formation. This is certainly a consequence of the moderate reaction temperature. Furthermore, after the harsh calcination procedure, our zeolite samples contain only a very low quantity of Brønsted acid centers. As the number of BAS directly controls the extent of carbonization [45] their absence is certainly an advantage as long as only the redoxactive properties are of interest.

Unfortunately it was not yet possible to determine the reaction products of the system because they could not be distilled off the zeolite. A GC/MS analysis of products extracted with a suitable solvent proved mainly oligomeric DMHD species which have to be assigned to a chain reaction of DMHD radical cations in the solvent, thus concealing other possible products in low concentrations. Further insight into the oxidation reaction may be obtained with a flow reactor together with an online analytical method. We expect hydroperoxides or cyclic peroxides as possible reaction products, in analogy to the photocatalytic work by Blatter, Frei and co-workers [40–42].

4. Conclusions and outlook

We have shown that the single-electron transfer in dehydroxylated zeolites may be used to develop a new concept for the functionalization of unsaturated hydrocarbons. We demonstrate that the active sites are neither Brønsted nor Lewis acid sites, and therefore call them single-electron transfer sites. The novel point is that these sites are catalytically active, as demonstrated by the continuous consumption of O_2 with up to 4000 cycles per active site and the recovery of the radical cation signal after the oxygen has been used up. We are not aware that such an observation has been made before by ESR. The results suggest that it may be possible to design closed-loop catalytic chemical reactions in which radical cations are activated intermediates. Since catalytic oxidation is one of the key reactions for providing economic benefits [46,47] it would be highly attractive to have a reaction that works with molecular oxygen in place of the more expensive peroxides. Further work is needed to extract and identify the products and to increase the turnover number.

Acknowledgments

The authors are greatly indebted to Dr. J. Opitz (Institute of Organic Chemistry, University of Stuttgart) for mass spectra and valuable advice and to Prof. G. Engelhardt (Institute of Technical Chemistry, University of Stuttgart) for NMR spectra and fruitful discussions. We further thank CU Chemie Uetikon for providing us with the zeolites.

References

[1] H.G. Karge, M. Hunger, H.K. Beyer, in: L. Puppe, J. Weitkamp (Eds.), Catalysis and Zeolites—Fundamentals and Applications, Springer, Berlin, 1999, p. 198.
[2] R. von Ballmoos, D.H. Harris, J.S. Magee, in: G. Ertl, H. Knözinger, J. Weitkamp (Eds.), Handbook of Heterogeneous Catalysis, vol. 4, Wiley–VCH, Weinheim, 1997, p. 1955.
[3] J.A. Martens, P.A. Jacobs, Stud. Surf. Sci. Catal. 137 (2001) 633.
[4] J.B. Uytterhoeven, L.G. Christner, W.K. Hall, J. Phys. Chem. 69 (1965) 2117.
[5] H.A. Szymanski, D.N. Stamires, G.R. Lynch, J. Opt. Soc. Am. 50 (1960) 1323.
[6] G.H. Kühl, in: J.B. Uytterhoeven (Ed.), Proc. 3rd Int. Conf. Molecular Sieves, Zürich, Recent Progress Reports, Univ. of Leuwen Press, Leuwen, 1973, p. 227.
[7] G.H. Kühl, J. Phys. Chem. Solids 38 (1977) 1259.
[8] P.A. Jacobs, H.K. Beyer, J. Phys. Chem. 83 (1979) 1174.
[9] G.H. Kühl, in: L. Puppe, J. Weitkamp (Eds.), Catalysis and Zeolites—Fundamentals and Applications, Springer, Berlin, 1999, p. 81.
[10] H. Garcia, H.D. Roth, Chem. Rev. 102 (2002) 3947.
[11] A. Corma, H. Garcia, Chem. Rev. 102 (2002) 3837.
[12] X. Liu, J.K. Thomas, Langmuir 9 (1993) 727.
[13] S. Shih, J. Catal. 79 (1983) 390.
[14] C.J. Rhodes, Colloids Surf. A 72 (1993) 111.
[15] F.R. Chen, J.J. Fripiat, J. Phys. Chem. 96 (1992) 819.
[16] R. Crockett, E. Roduner, Stud. Surf. Sci. Catal. 84 (1994) 527.
[17] J.-P. Lange, A. Gutsze, H.G. Karge, J. Catal. 114 (1988) 136.
[18] H.G. Karge, J.-P. Lange, A. Gutsze, M. Łaniecki, J. Catal. 114 (1988) 144.
[19] A. Corma, A.V. Orchillés, Micropor. Mesopor. Mater. 35 (2000) 21.
[20] T. Leu, E. Roduner, Stud. Surf. Sci. Catal. 135 (2001) 13-P-08.
[21] J.L. Franklin, A. Mogenis, J. Phys. Chem. 71 (1967) 2820.
[22] E. Roduner, R. Crockett, L.-M. Wu, J. Chem. Soc., Faraday Trans. 89 (1993) 2101.
[23] H.G. Karge, J. Weitkamp, Chem.-Ing.-Tech. 58 (1986) 946.
[24] H.G. Karge, Z. Phys. Chem. (N.F.) 76 (1971) 133.
[25] H.G. Karge, Z. Phys. Chem. (N.F.) 122 (1980) 103.
[26] H.G. Karge, H.K. Beyer, G. Pál-Borbély, Catal. Today 3 (1988) 41.
[27] T. Takaishi, A. Yusa, Y. Ogino, S. Ozawa, Jpn. J. Appl. Phys., Suppl. 2 (1974) 279.
[28] G. Garralón, A. Corma, V. Fornés, Zeolites 9 (1989) 84.
[29] M. Niwa, M. Iwamoto, K.-I. Segawa, Bull. Chem. Soc. Jpn. 59 (1986) 3735.
[30] E.E. Senderov, A.M. Bychkov, I.V. Mishin, A.L. Klyachko, H.K. Beyer, Stud. Surf. Sci. Catal. 49 (1989) 355.
[31] L.C. Jozefowicz, H.G. Karge, E.N. Coker, J. Phys. Chem. 98 (1994) 8053.
[32] B. Hunger, H. Miessner, M. von Szombathely, E. Geidel, J. Chem. Soc., Faraday Trans. 92 (1996) 499.
[33] A.L. Klyachko, T.R. Brueva, I.V. Mishin, G.I. Kapustin, A.M. Rubinstein, Acta Phys. Chem. (Szeged) 24 (1978) 183.
[34] N. Cardona-Martínez, J.A. Dumesic, Adv. Catal. 38 (1992) 149.
[35] B. Hunger, J. Hoffmann, P. Mothsche, J. Therm. Anal. 32 (1987) 2009.
[36] J.-V. Folgado, H. Garcia, V. Martí, M. Esplá, Tetrahedron 53 (1997) 4947.
[37] I. Balint, M.-A. Springuel-Huet, K. Aika, J. Fraissard, Phys. Chem. Chem. Phys. 1 (1999) 3845.
[38] P.J. Gellings, H.J.M. Bouwmeester, Catal. Today 58 (2000) 1.
[39] P. Kubánek, B. Wichterlová, Z. Sobalík, J. Catal. 211 (2002) 109.
[40] H. Frei, F. Blatter, H. Sun, CHEMTECH 26 (1996) 24.
[41] F. Blatter, H. Sun, S. Vasenkov, H. Frei, Catal. Today 41 (1998) 297.
[42] H. Frei, F. Blatter, H. Sun, US Patent 5,827,406 (1998) and 5,914,013 (1999).
[43] M. Che, A.J. Tench, Adv. Catal. 32 (1983) 1.
[44] J.H. Lunsford, Catal. Rev. 8 (1973) 135.
[45] H.G. Karge, E.P. Boldingh, Catal. Today 3 (1988) 53.
[46] National Institute of Standards and Technology, Advanced Technology Program; URL: http://www.atp.nist.gov/atp/97wp-cat.htm.
[47] American Chemical Society, Industrial and Engineering Chemistry Division; URL: http://membership.acs.org/i/iec or http://www.ccrhq.org/vision.